Received: 10 May 2021 | Revised: 29 September 2021 | Accepted: 10 October 2021

DOI: 10.1002/jez.b.23100

RESEARCH ARTICLE

JEZ-B MOLECULAR AND DEVELOPMENTAL EVOLUTION WILEY

Segment number threshold determines juvenile onset of germline cluster expansion in *Platynereis dumerilii*

Emily Kuehn[1,2] | **David S. Clausen**[3] | **Ryan W. Null**[1] | **Bria M. Metzger**[1] | **Amy D. Willis**[3] | **B. Duygu Özpolat**[1]

[1]Bell Center for Regenerative Biology and Tissue Engineering, Marine Biological Laboratory, Woods Hole, Massachusetts, USA

[2]Evolutionary Biology Centre, Uppsala University, Uppsala, Sweden

[3]Department of Biostatistics, University of Washington, Seattle, Washington, USA

Correspondence
B. Duygu Özpolat, Bell Center for Regenerative Biology and Tissue Engineering, Marine Biological Laboratory, Woods Hole, MA 02543, USA.
Email: dozpolat@mbl.edu

Funding information
National Institute of General Medical Sciences, Grant/Award Numbers: R35GM133420, R35GM138008

Abstract

Development of sexual characters and generation of gametes are tightly coupled with growth. *Platynereis dumerilii* is a marine annelid that has been used to study germline development and gametogenesis. *P. dumerilii* has germ cell clusters found across the body in the juvenile worms, and the clusters eventually form the gametes. Like other segmented worms, *P. dumerilii* grows by adding new segments at its posterior end. The number of segments reflect the growth state of the worms and therefore is a useful and measurable growth state metric to study the growth-reproduction crosstalk. To understand how growth correlates with progression of gametogenesis, we investigated germline development across several developmental stages. We discovered a distinct transition period when worms increase the number of germline clusters at a particular segment number threshold. Additionally, we found that keeping worms short in segment number, by manipulating environmental conditions or via amputations, supported a segment number threshold requirement for germline development. Finally, we asked if these clusters in *P. dumerilii* play a role in regeneration (as similar free-roaming cells are observed in *Hydra* and planarian regeneration) and found that the clusters were not required for regeneration in *P. dumerilii*, suggesting a strictly germline nature. Overall, these molecular analyses suggest a previously unidentified developmental transition dependent on the growth state of juvenile *P. dumerilii* leading to substantially increased germline expansion.

KEYWORDS
annelida, critical size, developmental transition, gametogenesis, sexual reproduction

1 | INTRODUCTION

Sexual maturation is one of the major developmental transitions in an animal's life history. Maturation requires production of gametes (eggs and/or sperm) via a process called gametogenesis. The onset and progression of gametogenesis are tightly coupled with the growth and nutritional state of an individual. Therefore growth, nutritional state, and sexual reproduction are intertwined (Lord & Shanks, 2012). Animals have mechanisms that assess body size and regulate processes such as gametogenesis as a result of the systemic check and feedback (Hyun, 2018; Lui & Baron, 2011). For example, in *Drosophila* and *C. elegans*, nutritional status and insulin signals affect germline

stem cell (GSC) division rate and gamete production (Hubbard et al., 2013; Narbonne & Roy, 2006; Shim et al., 2013). In holometabolous insects, reaching a critical weight is required for the transformation from an immature form to an adult (metamorphosis) which will reproduce sexually (Tennessen & Thummel, 2011). This somatic-germline crosstalk and the regulation of maturation based on body weight and size has been extensively studied in many insects and other ecdysozoans, which have stepwise (discontinuous) growth with molting and/or metamorphosis (Hutchinson et al., 1997; Sebens, 1987). However, there is much less information available on how growth and nutritional status affects developmental transitions in invertebrates which display continuous growth, such as annelids (segmented worms), planarians, and tunicates.

Annelids have repeating body parts called segments. Most annelids grow continuously by adding segments at their tail end throughout their lives. As a result, growth can be easily measured by counting the number of chaetigerous segments (segments that have bristles, aka. setigers) and correlations can be made with developmental transitions and stages of sexual maturation. We use the polychaete *Platynereis dumerilii* as a model system (Özpolat et al., 2021) for studying germline formation, gametogenesis, and germline regeneration. *P. dumerilii* has four primordial germ cells (PGCs) that are set aside during embryogenesis (Özpolat et al., 2017; Rebscher et al., 2007, 2012; Rebscher, 2014; Zelada González, 2005). The PGCs are quiescent until they migrate anteriorly (Figure 1a,b) where they start proliferating and form a cluster (anterior cluster, Figure 1c) located right behind the jaws (segments 4–5 in younger juveniles). They express germline markers such as *vasa*, *piwi*, *nanos*, and express the Vasa protein (Figure 1d′). As the worms grow, the anterior cluster is thought to give rise to cells that migrate posteriorly to the trunk segments and form many small gonial clusters spread across the coelomic cavity, the parapodia (appendages on each side of a segment), and around the gut (Zelada González, 2005) (Figure 1d,d′). *P. dumerilii* does not have centralized somatic gonads, and these clusters eventually give rise to the gametes (Fischer, 1974, 1975; Meisel, 1990) (Figure 1e). The worms have separate sexes, and upon the completion of sexual maturation, males and females are easy to differentiate from each other based on external morphology and presence of fully mature gametes. Overall, the behavior of the 4 PGCs in the early larval stages, and the later stages of gametogenesis in the older juveniles have been well-documented (Figure 1a,b and 1e) (Fischer, 1974, 1975; Meisel, 1990; Özpolat et al., 2017; Rebscher et al., 2007, 2012; Rebscher, 2014; Zelada González, 2005). However, there is less documentation for the earlier gametogenesis stages, namely the formation of the numerous small *vasa*+ gonial clusters that populate the coelomic cavity during the mid-juvenile stages (Figure 1c,d).

Gametogenesis in many animals comprises a wide range of events: first, PGCs proliferate via mitosis to increase their numbers and produce gonial cells (spermatogonia and oogonia). These gonial cells may continue to multiply via mitosis and eventually differentiate into primary oocytes and primary spermatocytes. At this stage meiosis starts, and in parallel other gamete maturation processes such as vitellogenesis in oocytes take place. These processes culminate in the production of mature oocytes and sperm (Giese & Pearse, 1974; Nieuwkoop & Sutasurya, 1981). In *P. dumerilii*, detailed work has been carried out on the late stages of gametogenesis using TEM and other histological techniques (Fischer, 1974, 1975; Hauenschild & Fischer, 1969; Hempelmann, 1911; Meisel, 1990). These studies investigated worms that are 50 segments or longer, in which gamete maturation has already begun.

In *P. dumerilii*, earlier stages of gametogenesis have been neglected, as without molecular markers, the coelomic gonial clusters are hard to discriminate from the surrounding somatic cells. Because the early works predated the availability of molecular tools and markers, the early stages of gametogenesis when gonial clusters form and populate the trunk segments in the immature juveniles were not investigated. More recently, molecular gene expression analyses have been carried out in *P. dumerilii* using several germline/multipotency markers (Rebscher et al., 2007, 2012; Zelada González, 2005). These works hinted at a connection between segment number and changes in gonial cluster distribution, but they did not systematically investigate juveniles to explore this correlation. Another recent study, which used contemporary molecular tools and gene knockouts, suggested coordination between energy metabolism, growth, and sexual maturation (Andreatta et al., 2020). However, this study also focused on later stages of sexual maturation in pre-mature worms. Overall, at what stage gonial clusters start populating the trunk segments, and whether there is a critical body size for this step of gametogenesis to get initiated have not been identified.

To address this knowledge gap, we analyzed the dynamics of *vasa*-expressing gonial clusters across developmental stages of the juvenile *P. dumerilii*. We found that the formation of *vasa*+ gonial clusters consistently occurs after worms have reached 35–40 chaetigerous segments in length. We show that the chronological age of the worms is a poor predictor of the number of gonial clusters a worm would have. This indicates that gametogenesis in *P. dumerilii* is tightly coupled with growth and not age, and there appears to be a critical size (in terms of segment number) that needs to be reached for progression of gametogenesis. This molecular and quantitative approach allowed us to determine a developmental stage transition that was not identified before. We propose the 35–40 segment growth phase to be a major developmental transition in this species. These analyses will facilitate further investigations of gametogenesis as well as the response of the germline to body size during regeneration, and will help clarify the relationship between growth and sexual maturity in this semelparous organism with indeterminate growth.

2 | MATERIALS AND METHODS

2.1 | GitHub resources for this publication

We have uploaded R code, associated spreadsheets, protocols, and additional resources related to the work reported here on GitHub to a specific repository for this manuscript (ÖzpolatLab-GitHub-Kuehn, 2021; ÖzpolatLab-HCR, 2021).

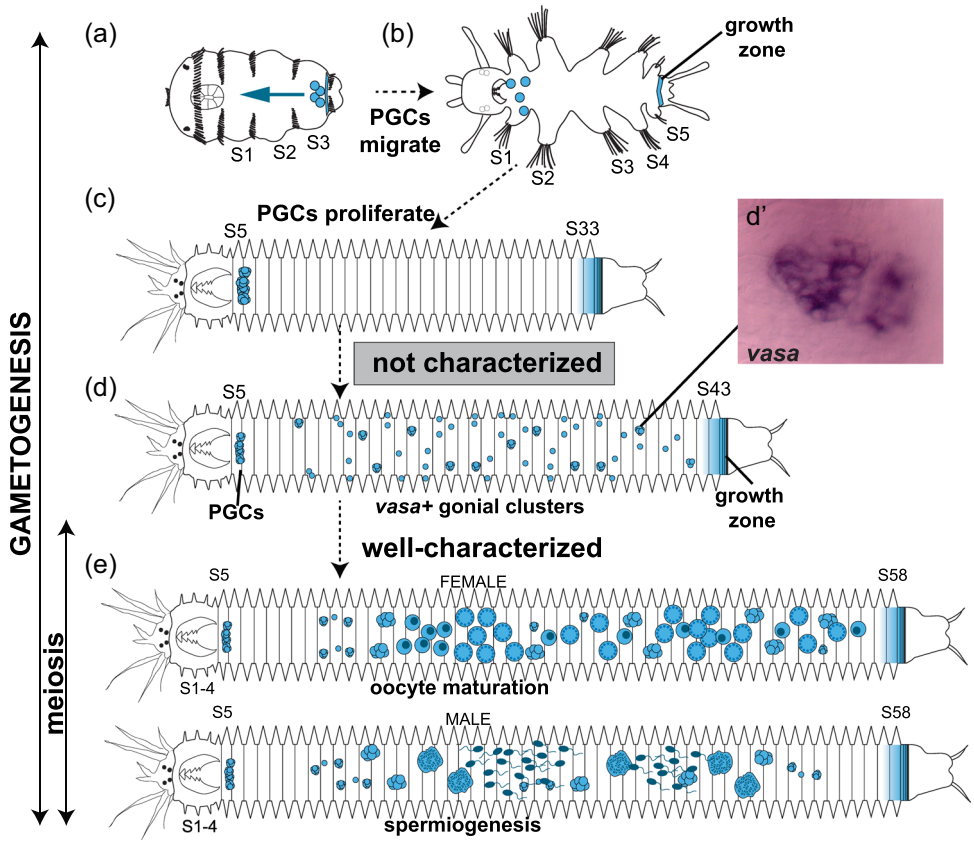

FIGURE 1 Schematics of gametogenesis in *Platynereis dumerilii*. (a) 3-segmented larval *P. dumerilii* has 4 PGCs (4 blue circles) located next to the growth zone (blue stripe to the right of 4 PGCs) at the tail. (b) By the time the larva grows into 5 segments, 4 PGCs migrate anteriorly (indicated by blue arrow in A). (c) In juvenile worms these cells proliferate and form a large cluster in the anterior segments 5-6. (d) Many small clusters that later appear in posterior trunk segments. These are thought to come from the large anterior cluster in segments 5-6. The correlation between the total segment number and gonial cluster formation has not been resolved. (d′) Example of a gonial cluster in the trunk segments showing *vasa* mRNA via in situ hybridization. (e) In pre-mature worms, later stages of gametogenesis have been better documented. These are the stages when maturing sperm and oocytes can be observed without requiring any molecular markers because they are easy to distinguish based on cell morphology even by simple light microscopy. S: segment. mRNA, messenger RNA

2.2 | Animal culturing

Animals were raised in conditions as described previously (Kuehn et al., 2019) except where noted below. Briefly, all the samples used in this study were kept at light/dark photoperiodic conditions of 16:8 h, and 8 days of moonlight at night every 28 days.

2.3 | Whole mount in situ hybridizations (WISH)

We followed the published WISH protocols with the following modifications (Gazave et al., 2013; ÖzpolatLab-GitHub-Kuehn, 2021): Briefly, animals were fixed in 4% paraformaldehyde at 4°C overnight, transferred stepwise into 100% methanol, and kept at −20°C until the start of WISH procedure. Samples were rehydrated through a methanol/DEPC-treated PBSt series. They were then digested in 0.1 mg/ml Proteinase K (Ambion AM2548) for 5 min at room temperature before being briefly (<1 min) washed in a glycine (2 mg/ml) DEPC-PBSt solution, and refixed in 4% paraformaldehyde for 30 min on ice. Dig-labeled sense and antisense RNA probes for *vasa* were prepared as described previously (Gazave et al., 2013) (Ambion AM1310, Roche 11277073910). Probes were diluted to 2 ng/µl in 100% hybridization solution, and were denatured at 85°C for 10 min. Samples were then incubated in the probe solution at 65°C overnight (approximately 16 h). Final colorimetric reaction was developed using NBT/BCIP substrate. Keeping most samples in NBT/BCIP overnight typically provided enough time for the signal to develop with minimal background. Samples were washed twice with stop buffer to end the reaction and at least three times in PBSt (30 min each) while being kept on ice and on a nutator. Samples were then transferred into 75% glycerol/25% PBSt stepwise and stored (protected from light) at −20°C until imaging. Sense probe controls were included in each experiment to account for background staining. Full protocol is provided in the GitHub repository (ÖzpolatLab-GitHub-Kuehn, 2021).

2.4 | Hybridization chain reaction (HCR)

Probe (oligo pool) design: Based on the split-probe design of HCR3.0 reported previously (Choi et al., 2014, 2018), we wrote a custom software (ÖzpolatLab-HCR, 2021) to create 30 DNA oligo probe pairs specific to *P. dumerilii vasa* messenger RNA (mRNA) (Genbank Accession: AM114778.1). For each probe pair, the software takes a 52 bp footprint from the input complementary DNA sequence, using the 25 nucleotides at the 5′ and 3′ ends as the antisense complement of the RNA target sequence, the intervening 2 bp is left unpaired as a buffer region between the pair. The algorithm then skips ≥2 bp 3′ of the previous probe pair and repeats the creation of a new probe pair. Finally, one half of the B1 initiator (B1I1 or B1I2) is appended to each oligo in a pair, such that each pair has a complete B1 initiator sequence between the two of them. Exact oligo sequences and the associated hairpins are listed in the Supporting Information File. The sequences generated by the software were used to order a single, batched DNA oligo pool (50 pmol DNA oPools Oligo Pool) from Integrated DNA Technologies, resuspended to 1 pmol/µl in 50 mM Tris buffer, pH 7.5.

2.4.1 | Tissue collection and HCR

Samples for HCR were fixed the same way as the WISH samples explained above and stored in 100% Methanol at −20°C until the procedure. Probe hybridization buffer, probe wash buffer, amplification buffers, and a DNA HCR amplifier hairpin set were purchased from Molecular Instruments (https://www.molecularinstruments.com/). The sequence for the HCR B1 amplifier has been reported previously (Choi et al., 2014) (see Supporting Information File). HCR was performed according to the published methodology (Choi et al., 2018). To suit our samples, steps from tissue rehydration through to post-fixation were performed in six-well plates according to standard *P. dumerilii* colorimetric WISH protocols (ÖzpolatLab-GitHub-Kuehn, 2021). All subsequent steps were performed in 2 ml tubes. The wash volume was decreased from 2 ml to 800 µL to accommodate less tissue and conserve reagents. Incubation volumes were maintained. At the amplification step, DAPI was added to a final concentration of 2 µg/ml. Full protocol is provided in the GitHub repository (ÖzpolatLab-GitHub-Kuehn, 2021).

2.4.2 | Imaging

HCR samples were mounted in Slowfade Glass with DAPI (Thermo S36920-5X2ML), kept at 4°C until imaging, and imaged using Zeiss Laser Scanning Confocal Microscope LSM 780. Images were processed for levels in FIJI (Schindelin et al., 2012).

2.5 | Scoring control samples for *vasa*+ clusters

We culture worms in plastic boxes labeled with the date of birth of a given batch, therefore the chronological age of any worm in our cultures is known at the time of fixation. We scored each worm sample for the total number of chaetigerous segments and the total number of *vasa*+ clusters. For assembling this dataset, we collected and fixed worms at a range of chronological ages (36–340 days post-fertilization) and a range of segment numbers (10–70 segments), then processed and analyzed them for the *vasa* expression phenotypes. We have also included control worms from other experiments into this dataset (Dataset-01). More than 400 control worms were scored.

For scoring, samples were imaged using a Zeiss V20 stereoscope (except for the high magnification images, which were acquired using a Zeiss M2 upright compound scope). Scoring was then carried out on the images by counting the number of segments and *vasa*+ clusters on each sample by using the count tool in Adobe Photoshop or the cell counter plug-in in FIJI (Schindelin et al., 2012). Examples have been uploaded to Zenodo (ÖzpolatLab-GitHub-Kuehn, 2021) (doi.org/10.5281/zenodo.4587817, doi.org/10.5281/zenodo.4587804). The following criteria were used for scoring: (i) *vasa*+ gonial clusters were identified by their distinctive dark staining and well-defined borders. However, to avoid false positives, clusters that were located in parts of the worm containing large amounts of gut content were not counted. Likewise, clusters located in the parapodia that displayed similarity to the background signal in the sense controls were not counted. (ii) the anterior cluster and any clusters near the head segments that looked like could be a part of the anterior cluster (~first six segments) were not included. In all the scatter plots, the cluster numbers exclude the anterior cluster. (iii) Positive clusters were identified as strongly stained single cells or globular clusters of multiple cells. For simplicity, we refer to anything that was counted as positive for the *vasa*+ marker and received a scoring point as a "cluster". Although some clusters consisted of multiple cells, it was not possible to count the exact number of cells in each cluster. If clusters appeared to be touching but the overall shape indicates that there were at least two clusters, these were counted as two separate clusters. (iv) For counting segments, presence of chaetae was deemed sufficient to count a segment, including for the young segments at the posterior end. Each bilateral pair of parapodia was considered to be one segment. (v) During dehydration-rehydration and WISH, sometimes the tails broke. Any worms with tails that had broken off during the WISH procedure or tails that looked like they were regenerating in the control group were also removed from the data pool to prevent uncertainty about the number of segments a broken sample had. (vi) Samples that showed signs of metamorphosis and full maturation (color change, loss of gut) were not included in scoring.

2.6 | High versus low populations density experiments

A fertilization batch consisting of full and half-sibling worms was kept in a large culture box (35.6 × 27.9 × 8.3 cm, *Sterilite*, 1963) in 1500 ml natural filtered seawater (NFSW) from the time of fertilization until 6 weeks post-fertilization. At this time, four low density and four high density cultures were established by transferring worms from the

original culture into separate small boxes (27.9 × 16.8 ×7 cm, *Sterilite*, 1961) in 500 ml NFSW. High density cultures consisted of 100 worms per box while low density cultures consisted of 20 worms per box. Half of all low- and high-density boxes received the normal amount of food per worm (0.57 mg of spirulina/sera micron mixture per worm) each time they were fed. Remaining cultures received half of the normal amount of food (0.28 mg). All culture boxes were fed three times per week (Monday, Thursday, and Saturday) and before each feeding, the seawater in each box was changed to prevent fouling (also Monday, Thursday, and Saturday). A whole box from each group (high or low) and feeding regimen (normal or underfed) was collected and fixed for WISH after 2 and 4 weeks in these conditions (i.e., 8 and 10 weeks post-fertilization). Worms from the original culture were fixed at the time the new high- and low-density boxes were established ($t = 0$).

2.7 | P10–P20 amputation experiment

Before amputation, worms were anesthetized in a 1:1 mixture of 0.22 µm NFSW and 7% MgCl2 until no movement was observed when prodded (approximately 5–10 min). The segment number was determined by counting lateral pairs of parapodia. Amputations were made after the 10th (P10) or 20th (P20) segment by making a transverse cut using a scalpel (Dynarex 4115). Worms were washed in 0.22 µm-filtered NSW and placed into clean small (27.9 × 16.8 × 7 cm, *Sterilite*, 1961) culture boxes. The samples were fixed at the following time points: Day 0 (no amputation), 3 days post-amputation (dpa), 5, 7, 14, 20, 25, 30, 45, and 60 dpa. Among these time points, 14 dpa and older were used for the P10–P20 amputation analyses. Examples from all the time points, (including samples earlier than 14 dpa) were used for the regeneration analyses.

2.8 | Plots and statistical analyses

2.8.1 | Scatter plots and boxplots

Scatter plots and boxplots were generated either in RStudio (R Core Team, 2020; RStudio Team, 2020) or Microsoft Excel. The visuals were amalgamated and edited in Adobe Illustrator for clarity, shape and text size adjustments. All R scripts and datasets (01, 02, 03) are available as Supporting Information Material via GitHub (ÖzpolatLab-GitHub-Kuehn, 2021).

2.8.2 | Regression analyses of control samples for *vasa*+ clusters (Dataset-01)

To estimate the conditional median number of *vasa*+ clusters at each observed number of segments, we fit an isotonic median regression via the gpava function in the isotone R package (de Leeuw et al., 2009). In our analysis, we excluded observations for which worms broke before measurement of *vasa*+ cluster and segment number, as well as two observations for which age and/or posterior *vasa*+ cluster count was missing. We constructed 95% pointwise confidence intervals for the conditional median via a cluster bootstrap. The clusters were defined by the culture boxes in which each worm was grown to account for within-culture box dependence. We used 10,000 bootstrap iterations, and applied the correction given in Table 1 by Abrevaya et al (Abrevaya, 2005).

2.8.3 | Regression analyses of P10–P20 amputation experiment (Dataset-03)

In this experiment, the relationship between segment number and conditional median number of *vasa*+ clusters were compared across three conditions: control condition, worms after the 10th segment (P10) and worms amputated after the 20th segment (P20). We excluded all observations on worms with broken tails ($n = 150$). While the probability of tail break is likely associated with the number of segments, we analyzed complete worms under the assumption that for worms of a given length, the number of *vasa*+ clusters is not associated with the probability of tail break. If this assumption holds, this missing data reduces our sample size ($n = 353$, after exclusions) but should not bias our estimates of the association between number of segments and conditional median number of *vasa*+ clusters. The total number of unamputated control, P10, and P20 worms were $n = 123$, $n = 101$, and $n = 129$, respectively. The number of samples per time point and condition ranged $n = 7$–33 (Table S1). For each of these conditions, we estimated conditional median *vasa*+ clusters via the gpava function in R package isotone and constructed 95% pointwise confidence intervals as described above, again with cluster resampling based on culture box.

3 | RESULTS

3.1 | Gametogenesis in the juvenile and mature *P. dumerilii*

To characterize the behavior of the *vasa*+ PGCs and gonial clusters across growth stages of juvenile *P. dumerilii*, we carried out whole-mount in situ hybridization for *vasa* (Figure 2). We found that juvenile worms that are 10–19 segments long only had a few cells (4 or more) arranged in an arch right behind the head region ($n = 30$) (Figure 2a,a′). These cells appeared to multiply as the worms reached a length of 20–29 segments ($n = 110$), forming a ring-like structure in many of the samples (Figure 2b,b′). Neither of these stages (Figure 2a,b) had any *vasa*-expressing cells in the other segments except in the arch-like formation behind the head at segments 4–6 and at the posterior growth zone (Figure 2c″). In the worms that were 30–39 segments long ($n = 76$), the ring structure turned into a broader band (Figure 2c,c′). In this group, worms longer than 35 segments started having few cells

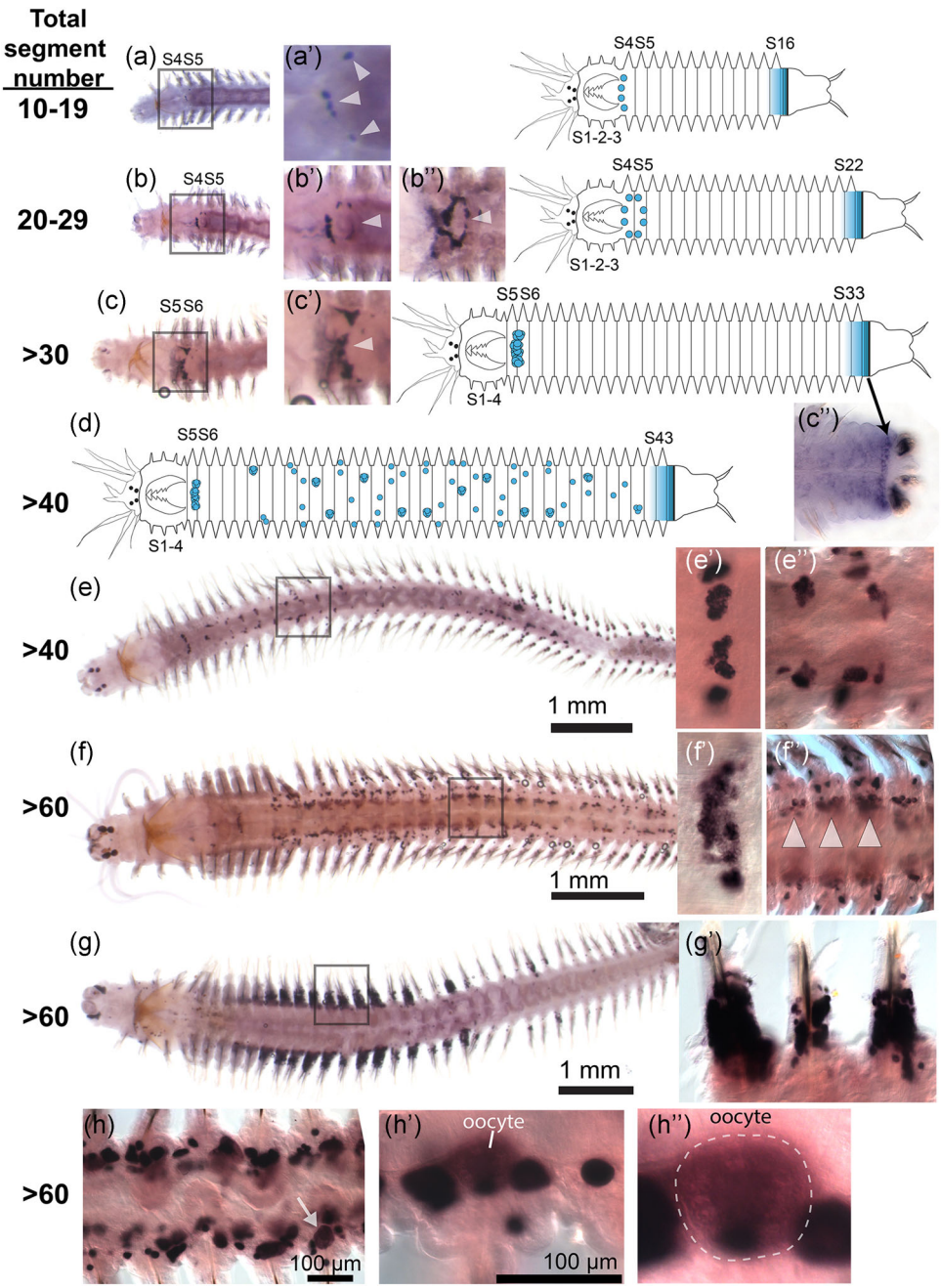

FIGURE 2 Gametogenesis in the immature juvenile and pre-mature *P. dumerilii*. (a) In worms between 10 and 19 segments in length, *vasa* positive cells can be found towards the anterior of the worm, just behind the jaws. (a′) Close-up of the anterior cluster in (a). (b) More *vasa* positive cells appear in a ring-like structure to encircle the esophagus as the worm grows. (b′) Close-up of the anterior cluster in (b). (b″) another example of the ring-like anterior cluster in a different sample. (c) *Vasa* expression continues to accumulate in this region in worms 30–39 segments long. (c′) Close-up of the anterior cluster in (c). (c″) *vasa* expression in the posterior growth zone. (d) Schematic of a worm longer than 40 segments with *vasa*+ gonial clusters (in blue) populating the trunk segments. (e) Clusters of *vasa*+ cells begin to appear throughout the posterior body cavity of the worm once it has reached 35–40 segments in length. (e–e″) Close-up views of the anterior cluster (e′) and trunk clusters (e″). (f) Clusters are more numerous in larger worms, and they start forming pockets (arrowheads in f″) that are regularly present in most segments. (f′,f″) Close-ups of anterior cluster (f′) and trunk clusters (f″). (g) *vasa* signal becomes localized in the anterior parapodia of some worms, and become completely absent in other regions. (g′) Close-up of parapodia showing localized expression in a sample similar to the one in (g). (h,h″) In some of these longer worms, immature oocytes are already present (arrowhead in h, and close-ups of an oocyte in h′ and h″). These oocytes are not yet fully mature, as evidenced by their diameter (much less than 160 µm, which is the diameter of a mature oocyte)

expressing *vasa* in the trunk region (Figure 4b). This pattern changed drastically as the worms reached lengths longer than 40 segments (40–49 segment-long; $n = 110$): most of the worms had numerous *vasa*+ cells and cell clusters scattered throughout the body (Figure 2d–f″, Figure 4b, Figure S1). In worms longer than 50 segments ($n = 168$), we observed a few different states. Many worms in this group had regularly spaced gonial clusters, especially in more anterior trunk segments (Figure 2f–f″). Meanwhile, in some samples we observed *vasa*+ oocytes at different stages of maturation ($n = 3$) (Figure 2h–h″), as well as samples that had *vasa* expression only in the parapodia ($n = 9$) (Figure 2g–g″). We think these latter animals may be males starting to make sperm as we never observe any oocytes in these samples. Sense controls showed an occasional striated background staining (Figure S4a′). Also note that the chaetal sacs in parapodia have a characteristic background staining in most juveniles usually in the more posterior segments (Figure S4a″). Overall, *vasa*+ gonial clusters in the trunk segments started appearing in worms 35 segments or longer, they became more prevalent once worms surpassed 40 segments in length, and in some worms longer than 60 segments, maturing gametes were evident.

P. dumerilii has separate sexes. Towards completion of sexual maturation, females and males obtain morphological characteristics and secondary sexual structures that make it easy to differentiate them. However, this is not possible to do in the immature (individuals with no visible maturing gametes), and pre-mature juveniles (visible maturing gametes that can be identified as oocytes or sperm in the coelom), which have very similar outside appearance in both sexes. We fixed female and male worms that started to mature sexually when maturation became morphologically distinguishable (males become white and red, females become yellow). Then we carried out traditional colorimetric in situ hybridization or HCR (a fluorescent mRNA detection procedure) for *vasa*. In samples processed for colorimetric in situ hybridization, 22 out of 34 female samples exhibited strong *vasa* signal in oocytes with *vasa* signal localized perinuclear in the oocytes (Figure 3a–c′). We confirmed this pattern of expression in the HCR-processed samples (Figure 3c,c′). Among the colorimetric in situ hybridization samples, there were also some females without any signal

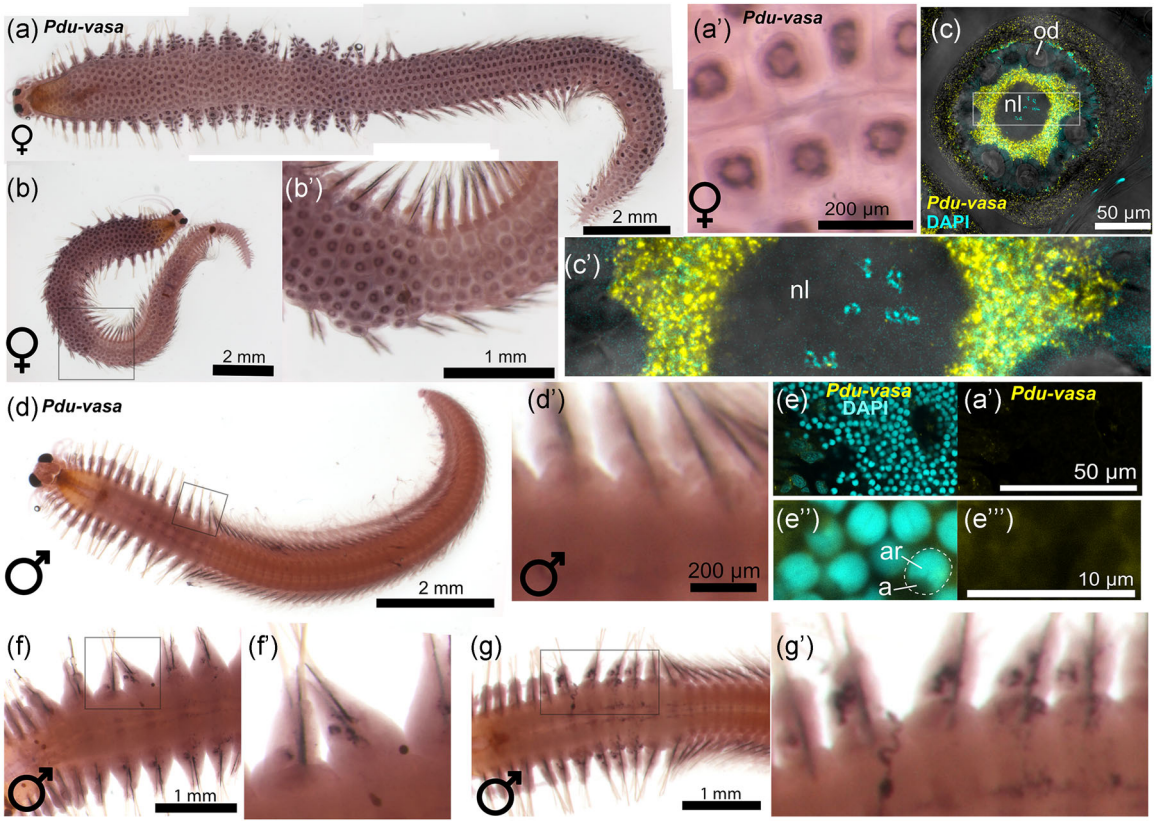

FIGURE 3 *vasa* expression in the mature female and males. (a–b′) Sexually mature females. Traditional whole mount in situ hybridization (WISH) shows *vasa* expression surrounding the nuclei of oocytes (a′ and b′). (c–c′) Fully mature oocyte processed for hybridization chain reaction (HCR) showing *vasa* mRNA expression (yellow) and nuclear stain DAPI (cyan) in the perinuclear region. Box in (c) indicates the magnified region in (c′). nl: nucleus, od: oil droplet. (d–d′) Sexually mature male shows no expression of *vasa*. However, depending on the level of maturation, some males still showed small patches of *vasa* positive regions (f–g′). (e–e‴) Spermatozoa in a fully mature male processed for HCR show no *vasa* signal. (e and e″) *vasa* in yellow and DAPI in cyan, merged. (e′ and e‴) *vasa* signal shown alone. The acrosome and axial rod can be noted in these magnified views. a: acrosome, ar: axial rod. (e″) and (e‴) are magnified views from (e) and (e)″. (f–g′) Additional samples that were mature males but had some patchy expression of *vasa*

(*n* = 12/34). While this may be due to a technical factor such as probe penetration issues, these samples may also reflect a stage, where detecting and/or visualizing vasa mRNA is harder because vasa mRNA may be too diffuse across the large oocyte volume. Indeed, we noticed gradations in the *vasa* signal that corresponded to how close a female was to spawning based on external morphology and oocyte maturation stage. Females with morphology consistent to that of worms ready to spawn (*n* = 22) (larger eggs, distinct atokous and epitokous parapodia) exhibited darker and perinuclear vasa signal compared to the females with less mature morphology (*n* = 6) that lacked the distinct *vasa* signal (Figure S2). This is supported by HCR results where we observed the *vasa* signal in fully mature female oocytes of HCR-processed samples (*n* = 2), but pre-mature females with oocytes still in maturation process (*n* = 4) did not have the concentrated perinuclear *vasa* signal, and instead showed a much more diffuse signal across the oocyte (Figure S3). In most males that were fully sexually mature based on external morphology, no signal for *vasa* expression was observed (Figure 3d–g′). However, there were some males with spotty signal in their parapodia (*n* = 13/54) (Figure 3f–g′), which may be some remaining gonial clusters that have not undergone spermatogenesis. We confirmed these results via HCR where no *vasa* signal was observed in the spermatozoa (Figure 3e–e‴). Sense controls showed no signal in oocytes or sperm (Figure S4b,c).

3.2 | *vasa*+ gonial cluster pattern is correlated with the total number of segments of individual worms

We next determined whether the chronological age (time since birth) or growth state (measured as total number of chaetigerous segments) of a worm had a greater effect on the progression of the pattern of *vasa*-expressing cells in the trunk. Specifically, we wanted to investigate when the switch from no *vasa* clusters to numerous *vasa* clusters happened. We hypothesized that if chronological age was the determining factor, worms would begin to produce *vasa*+ gonial clusters in the trunk at a set age regardless of size (in terms of segment number). If, however, chronological age was not critical, while reaching a particular growth state was the inducing factor for the *vasa* pattern, then we expected to see fast-growing worms develop *vasa*+ clusters more quickly relative to smaller worms of the same age.

To do this, we quantified the number of *vasa*+ gonial clusters in the trunk and the total number of segments for 494 individual worms of known chronological age (Figure 4). Gonial cluster counts excluded the anterior cluster (see Section 2, Figure 4a,a′). Plotting *vasa*+ gonial clusters by number of segments showed clear correlation (Figure 4b), while plotting *vasa*+ gonial clusters by age did not show a trend (Figure 4c). From the data it appears that most worms start forming *vasa*+ gonial clusters when they reach 30–40 segments. However, during this growth

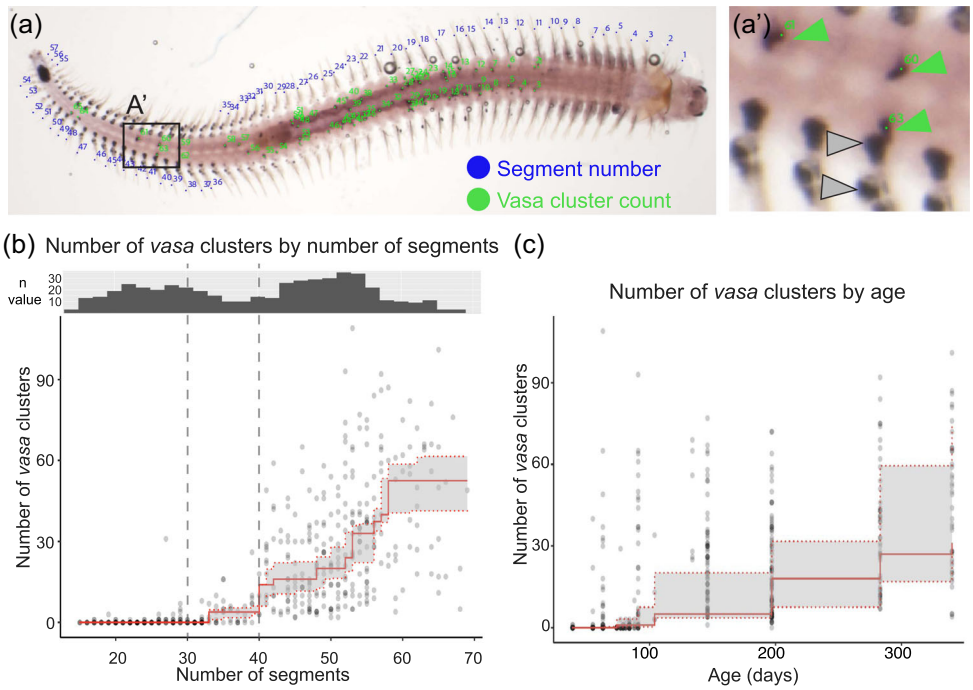

FIGURE 4 (a,a′) Example scoring of samples for segment number (blue) and *vasa* + clusters (green). (a′) Gray arrowheads— background, not scored; Green arrowheads—*vasa*+ clusters, scored. (b) Scatter plot showing the number of *vasa* clusters in worms by the number of segments at the time of fixation. Clusters typically begin forming after worms reach 30 segments and become numerous after approximately 40 segments. The estimated conditional median (red solid line) shows that this upward trend begins somewhere between 30 and 40 segments, closer to 35 segments. We also noted that there are no worms that are more than 40 segments in length that have zero *vasa* clusters in the trunk. The histogram above the scatter plot indicates the distribution of sample size by the number of segments in our dataset; notably, approximately half of the scored samples are below 40 segments and half are above. A 95% confidence interval for the conditional median is also indicated (gray shading between dashed red lines). (c) The same dataset and isotonic regression depicted in (b) but with median number of *vasa*+ clusters regressed on age. In contrast to segment number, age does not appear to be a strong determining factor for *vasa*+ cluster formation

stage, there were still numerous worms without any *vasa*+ gonial clusters in their trunk ($n = 41$). In contrast, all observed worms longer than 40 segments had *vasa*+ gonial clusters in the trunk region, and the clusters became numerous after this segment length (Figure 4b). Overall, these data suggest that *vasa*+ gonial clusters emerge according to the total segment number (growth) the worms have, and not based on their age (elapsed time since birth).

3.3 | High culture density slows down growth and delays *vasa*+ gonial cluster formation

We next tested whether culture density had any effect on the growth and gonial cluster formation by culturing worms in crowded or uncrowded conditions (100 worms in high density cultures and 20 worms in low density cultures). These cultures received the same amount of food per worm, were hosted in identical culture boxes, and overall kept under the same conditions except for the density of individuals in each box. We set the cultures up by splitting sibling worms into multiple high- or low-density cultures at 6 weeks post-fertilization (see Section 2 for details). Worms were cultured under these conditions for 2 weeks or 4 weeks, fixed, and processed for whole mount in situ hybridization to investigate the abundance of *vasa*+ gonial clusters (Figure 5a). In addition, 6-week-old control ($t = 0$) siblings were fixed at the start of the experiment (Figure 5a,b).

We found that in 2 weeks, all the worms in the low-density condition had developed several gonial clusters and were longer than 30 segments (Figure 5c′) while only a fraction of the high-density culture samples had this phenotype (Figure 5c). By 4 weeks under these conditions, most of the low-density worms had passed

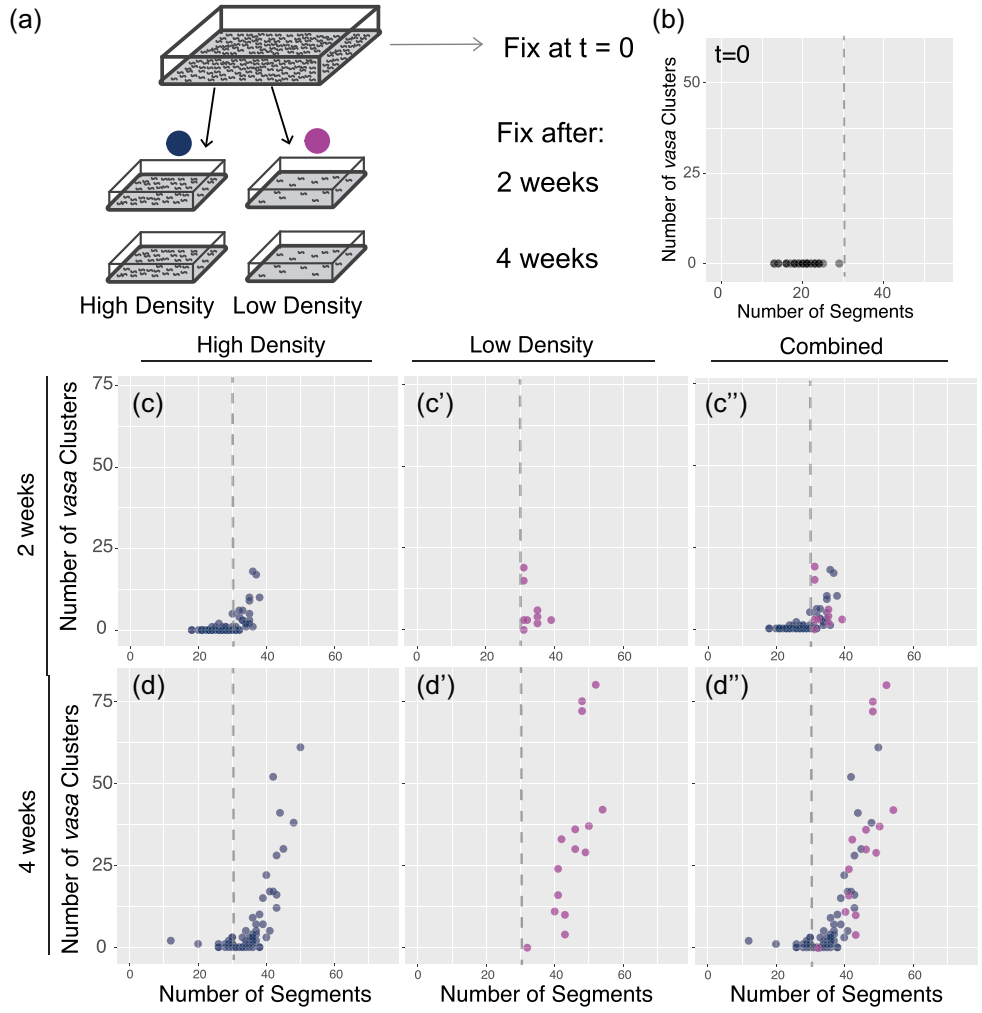

FIGURE 5 (a) Experiment schematic showing the establishment of four new culture boxes from one large high-density culture at 6 weeks post-fertilization ($t = 0$). Two low density (worms per box: $n = 20$) and two high density cultures (worms per box: $n = 100$) were created. One of each culture type was fixed at 2 and 4 weeks after the experiment was started. Some samples from the original culture were also fixed at $t = 0$. (b) Scatterplot showing number of *vasa*+ clusters and the number of segments per worm ($n = 39$) fixed at the beginning of the experiment at $t = 0$ (6 weeks post-fertilization). All the samples at $t = 0$ are shorter than 30 segments and have no *vasa*+ clusters in the trunk segments. (c–c″) Scatterplots showing the number of *vasa*+ clusters and the number of segments per worm 2 weeks after new low- and high-density cultures were established. (d–d″) Scatterplots showing the number of *vasa*+ clusters and the number of segments per worm 4 weeks after new low- and high-density cultures were established. Dashed line denotes 30 segment-length. Overall, irrespective of culture density, worms that reach 30 segments or longer start forming *vasa*+ clusters in the trunk

40 segments in length and developed numerous gonial clusters (Figure 5d′) while the high-density culture samples still had a larger fraction of worms below 40 segments (Figure 5d). We replicated these results using half the food volume per worm and found similar results (Figure S5). Overall, these results suggest that despite having the same relative amount of food available, worms in high density conditions grow slower than the worms in low density conditions. However, irrespective of culture density conditions, the gonial cluster formation still follows a similar pattern: when worms reach 30–40 segments the number of gonial clusters increase, and almost all the worms longer than 40 segments have gonial clusters in their trunk segments. Therefore, while culture density affects the rate of growth, it does not affect the body size threshold effect on the progression of gametogenesis.

3.4 | Removing segments via amputation delays the *vasa*+ gonial cluster formation

Keeping worms in high density cultures slowed down growth, thus allowing us to examine the relationship of size to the production of the *vasa*+ gonial clusters. However, this experiment did not differentiate between whether worms were counting the total number of segments they generated since birth or whether reaching a particular growth state (i.e., minimum body size measured by number of segments) is enough for triggering the phenotype of having abundant *vasa*+ gonial clusters. To test this, we performed a series of tail amputation experiments to remove segments (i.e., to make shorter worms) and have worms generate new segments, while simultaneously keeping them below a certain segment number (Figure 6a).

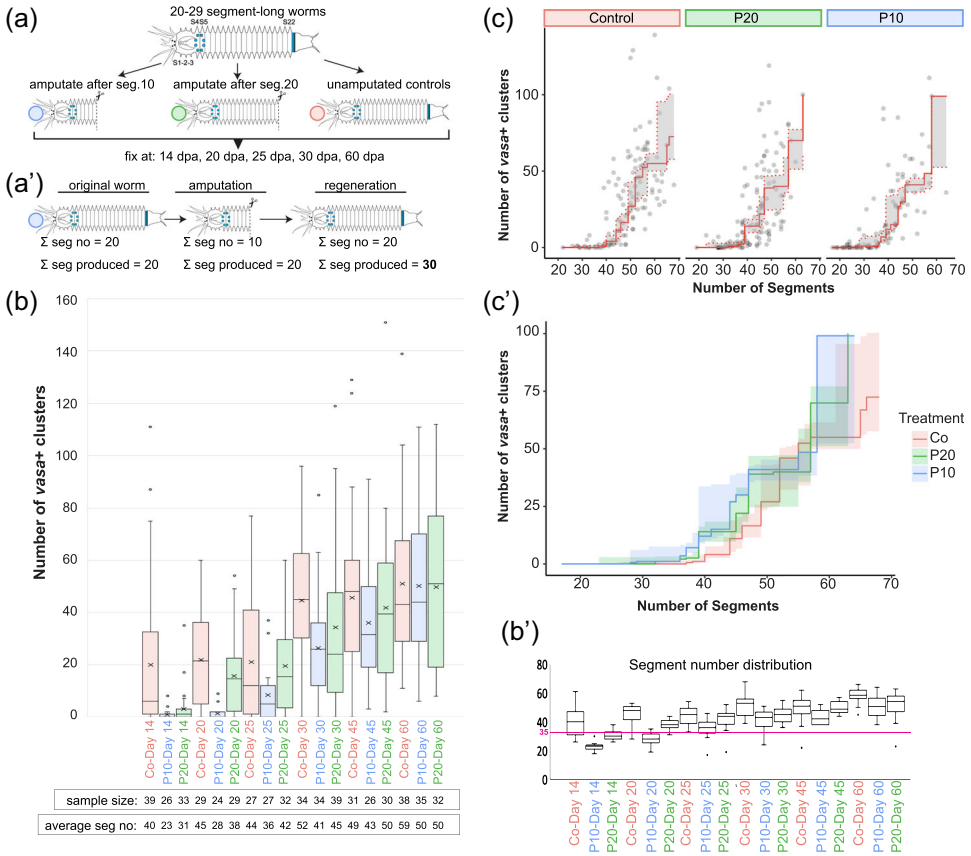

FIGURE 6 (a) Amputation experiment design featuring controls, worms cut after segment 10, and worms cut after segment 20. All groups were fixed at the listed time points. (a′) Examples of "current length" (∑ seg no) versus "total segment number produced" (∑ seg produced) during lifetime. Note that when a worm is amputated after segment 10, it has nevertheless produced 20 segments in its lifetime at the time of amputation. Once this worm regenerates 10 new segments, its current length is 20 segments, but total segment number produced during lifetime is 30. (b) Box plots showing the distribution of the number of *vasa*+ clusters per sample by time point and experimental condition. Sample size and average total segment number for each group are shown directly under the box plot labels. Note that the group amputated after segment 10 (P10) is delayed in forming numerous *vasa*+ clusters compared to P20 and control (which are longer in total segment number during the earlier time points). As individuals in group P10 reach 35 segments and longer, they start forming *vasa*+ clusters (starting Day 25). (b′) Segment number distribution for each group is shown. Magenta line denotes 35 segments, the size around which worms start showing an upward trend in forming *vasa*+ clusters. Note that group P10 reaches 35 segments at the Day 25 time point. (c,c′) Conditional median regression curves showing *vasa*+ cluster formation trends in each group, ignoring time, with 95% pointwise confidence intervals given by shaded regions (c′). All three lines show an upward trend around 35 segment-length, which suggests the worms need to reach this size threshold for forming *vasa*+ gonial clusters

These worms were the same age and were kept under the same culturing conditions, but were reduced in size via amputation.

We began the experiment with worms that were 10–20 segments long, so that we could reasonably assume that they did not yet have any *vasa*+ gonial clusters in the trunk (Figure 4b). We also fixed controls at the start (Day 0) of the experiment and verified that this was true for this batch of worms (Dataset 03). Worms were separated into three groups: controls, worms cut after segment #10 (P10), and worms cut after segment #20 (P20). A total of 30 worms in each group were fixed at different time points post-amputation (Figure 6a), processed for WISH for *vasa* expression, and were scored for the number of *vasa*+ gonial clusters as described previously. The two amputated groups (P10 and P20) also served as controls for each other in case amputation alone caused an effect. Worms fully regenerate and produce approximately 10 new segments by 14 days post-amputation (Figure 6b′).

If the worms "count" the total number of segments they have produced over their lifetime and trigger *vasa*+ gonial cluster production accordingly, we would expect to see a shift in the appearance of gonial clusters to lower segment numbers in amputated animals. For example, if a worm of 22 segments is amputated after segment 10, and regenerates 11 segments, it would have produced about 33 segments throughout its life (22 original + 11 regenerated), even though its current length would be 21 segments (10 remaining post-amputation + 11 new) (Figure 6a′). Therefore, if a worm simply needs to have produced 30–40 segments to start making gonial clusters, we would expect gonial clusters to begin to appear in this worm around the 20–30 segment length since this would be the number of total lifetime produced segments equivalent to 30–40. However, if having a minimum segment number (30–40 segments) at a given time is required for triggering the *vasa*+ cluster production, then we would expect to see a delay in amputated groups for producing *vasa*+ clusters until the worm reaches that segment threshold.

Both groups were found to fully regenerate and produce around 10 new segments by 14 days post-amputation (Figure 6b′). We found that amputated worms in both groups P10 and P20 showed a delay in developing gonial clusters compared with controls (Figure 6b). However, group P10 was more delayed than P20: for example, the majority of P20 samples fixed at Day 20 of the experiment already started having gonial clusters while P10 samples at this time point were still mainly lacking *vasa*+ clusters (Figure 6b). In all groups, as the worms get to the 30–40 segment threshold, they start forming gonial clusters (Figure 6b,b′). To verify that the two experimental groups follow a similar trend compared with controls in terms of number of segments by the number of *vasa*+ clusters, we carried out isotonic median regression analyses (Figure 6c,c′). We found that when we remove the time component, the *vasa*+ cluster by segment curves are similar in all three groups: the trend curves show that once the experimental groups reach the similar segment numbers as controls, they have similar *vasa*+ cluster numbers. Therefore, the relationship between the number of segments and the median number of *vasa*+ clusters is not meaningfully different in each group. Overall, these results are consistent with the hypothesis that the instantaneous segment number is the driving factor for gonial cluster formation, not the cumulative number of segments a worm produced up to a certain time point.

3.5 | *vasa*+ gonial clusters are not required for regeneration

Some organisms such as *Hydra*, planarians, or acoels have pluripotent stem cells scattered around the body and express germline/multipotency genes (David, 2012; Gehrke & Srivastava, 2016; Shibata et al., 1999). These cells are required for regeneration in these organisms. Recognizing that it is possible for a subset of the *vasa*+ cells in *P. dumerilii* to be similar to pluripotent stem cells in other highly regenerative organisms, our next question was whether the clusters are required for regeneration in *P. dumerilii*. To address this, we analyzed the worms from the P10–P20 amputation experiment (Figure 7). These worms are within the 10–20 segment length range and, as a result, do not have any *vasa*+ clusters in their trunk region, but only have the anterior cluster in the head region (around segments 4–5). Therefore, if the worms needed the *vasa*+ trunk clusters to regenerate they would fail regeneration. Alternatively, they would have cells from the anterior cluster respond to amputation and migrate towards the wound site. As expected, all the amputated worms regenerated, and we did not observe any *vasa*+ cells in the trunk segments, suggesting that *vasa*+ cells did not migrate towards the blastema from the anterior cluster region (Figure 7b–d, i–k). In both groups, worms eventually formed *vasa*+ gonial clusters (Figures 6 and 7f,g,m,n). Overall, these analyses show that neither the anterior *vasa*+ cells nor the trunk *vasa*+ clusters are required for regeneration in *P. dumerilii*.

4 | DISCUSSION

4.1 | Gametogenesis in *P. dumerilii*

Gametogenesis in Nereididae including *P. dumerilii* has been extensively studied in juvenile worms that already have maturing oocytes that are 40 µm or more in diameter or gonial clusters that already show signs of spermatogenesis (Brafield & Chapman, 1967; Fallon & Austin, 1967; Hauenschild & Fischer, 1969; Hauenschild, 1974; Lawrence & Soame, 2009; Schroeder & Hermans, 1975). These stages typically correspond to worms that are longer than 50 segments (Fischer et al., 2010). Stages of oocyte and sperm maturation in these larger worms have been studied using bright field and electron microscopy (Fischer, 1974, 1975; Meisel, 1990). However, these studies predated the availability of molecular tools and therefore focused on stages of gametogenesis when it was more feasible to detect gonial clusters reliably (i.e., in worms longer than ~50 segments with maturing gametes). The availability of immunohistochemistry and in situ hybridization made it possible to investigate germline/multipotency (GMP) marker expression in

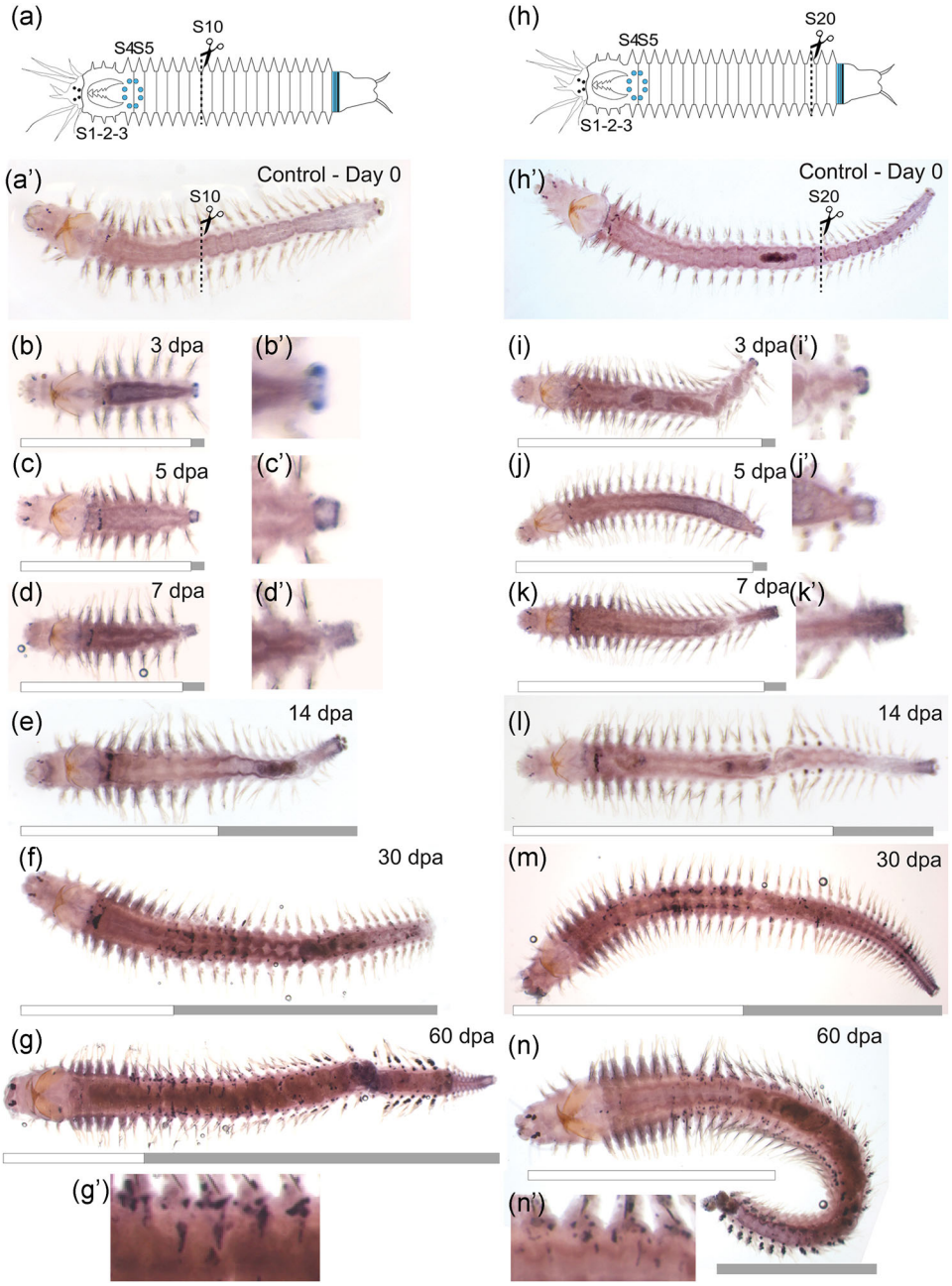

FIGURE 7 *vasa*+ cell clusters are not required for regeneration. (a,a′) and (h,h′) show amputation schematics and the control worms at the start of the experiment (Day 0). (b–g′) Worms amputated after segment 10, fixed at different time points and processed for WISH for *vasa*. (b′), (c′), and (d′) are close-ups of the regenerating tail in (b), (c), and (d). (i–n′) Worms amputated after segment 20, fixed at different time points and processed for WISH for *vasa*. (i′), (j′) and (k′) are close-ups of the regenerating tail in (i), (j), and (k). Up until 30 dpa time point, neither group has *vasa*+ clusters in the trunk region other than the anterior cluster in the segments right after the jaw. There is no evidence for *vasa*+ cell migration towards the blastema. However, all the samples regenerate successfully by forming a regeneration blastema which expresses *vasa* (b′–d′ and i′–k′). (g′) and (n′) are close-ups of *vasa*+ clusters in (g) and (n). Gray bars denote the regenerated region, while white bars denote the original segments. dpa: days post-amputation

P. dumerilii across different stages of development including embryonic, larval, and juvenile worms (Rebscher et al., 2007, 2012; Zelada González, 2005). However, a systematic analysis of formation of *vasa*+ gonial clusters in correlation with growth has not been carried out. Here, we addressed this knowledge gap and show that stages of gametogenesis in young juveniles are regulated by the growth state. Many previous studies in polychaetes used segment number as a metric, and this metric has been suggested as a staging system for juveniles in *P. dumerilii* previously as well (Fischer et al., 2010). Due to the wide variation in culture density and food availability across different studies, we suggest that chronological age is not a reliable method for staging

juveniles. Our study reinforces that reporting the total segment number of juvenile *P. dumerilii* samples is more informative of staging and may be necessary for the reproducibility in future studies.

4.2 | Gametogenesis and growth

In many animals, the PGCs give rise to GSCs, which in turn produce precursors that make the gametes (oocytes and sperm) (Nieuwkoop & Sutasurya, 1979, 1981). These processes are often regulated by growth factors and hormones such as insulin. Nutritional status and insulin-like growth factors affect GSC division rate in many organisms (Hubbard et al., 2013; Narbonne & Roy, 2006; Shim et al., 2013). For example, *C. elegans* has germline specific insulin-like genes regulating germline proliferation (Michaelson et al., 2010). Critical weight is required for metamorphosis in insects (Tennessen & Thummel, 2011) and growth abnormalities delay developmental transitions in *Drosophila* (Hariharan, 2012). Overall, growth, nutritional state, and sexual reproduction are intertwined (Hyun, 2018; Plaistow et al., 2004; Tharp et al., 2014).

The effects of hormones on growth, regeneration, and maturation have also been widely studied in *P. dumerilii* and other Nereididae (Andreatta et al., 2020; García-Alonso et al., 2011; Golding, 1967; Hofmann, 1976; Lawrence & Soame, 2009; Lidke et al., 2014; Schenk et al., 2016, 2019; Schroeder & Hermans, 1975). However, these works either focus on larval stages, or the later stages of gametogenesis in pre-mature worms already possessing maturing gametes. In previous studies, immature individuals were defined by no visible maturing gametes, while pre-mature adults have visible maturing gametes that can be identified as oocytes or sperm in the coelom. Finally, mature adults were defined as the fully metamorphosed and ready to spawn individuals (Schenk et al., 2019). Our results suggest the presence of an earlier developmental stage transition marked by the appearance of numerous gonial clusters and tightly coupled with growth. Whether there is some hormonal regulation triggering *vasa*+ gonial cluster formation in these younger immature juveniles is still unknown. It will be interesting to investigate if estradiol, methylfarnesoate, and gonadotropin-releasing hormones have a role during this developmental transition in the juveniles, as these hormones have been studied at other developmental stages in *P. dumerilii* (Andreatta et al., 2020; García-Alonso et al., 2011; Lidke et al., 2014; Schenk et al., 2016). For example, homozygous crz1/gnrhl1 knockout animals show a delay in maturation. While this delay could be explained by reduced growth phenotype these mutants have, it would be interesting to test if the mutants also have delayed formation of gonial clusters at the 35–40 segment size threshold. This could point out a decoupling of growth and gonial cluster formation. Similarly, methylfarnesoate, a member of the juvenile hormone family, has been identified as the brain hormone which has a role in regulating reproductive maturation (Schenk et al., 2016). Overall, expanding studies of gene and protein profiling (Schenk et al., 2019), and testing the effects of different hormones including within the context of ecotoxicology at this juvenile developmental transition stage will reveal whether these hormones play a role in the developmental switch to start proliferating gonial clusters.

4.3 | Effect of culture density on growth and gonial cluster formation

Organisms in juvenile stages tend to grow in size as they age and progress towards sexual maturation. Therefore, in individually-reared organisms while age can be an acceptable predictor and descriptor of growth state, for organisms that are reared in batch cultures, the population density (or stocking density) can often have an effect on growth due to many factors such as accumulation of waste products, competition for food, and release of inhibiting substances by the organisms themselves (Biswas et al., 2006; Dong et al., 2018; Tettelbach et al., 2011). Indeed, in our batch cultures, we often observe slower growth when worms are kept at high stocking density. We used these stocking density conditions as a way to slow down growth. We controlled for age by using worms from the same clutch, and we reared them in different stocking density conditions to test for the effect of growth rate on the *vasa*+ gonial cluster numbers in individual worms. Worms kept in high stocking density grew slower (they had a slower rate of segment addition) than the worms in low stocking density. The reasons for the difference in growth rate between the high and low stocking density groups remain unclear. In all these groups, food was standardized so each worm theoretically had access to the same amount of calories. However, in low density cultures, there was more space per worm compared to in high density cultures. Having the additional space may help worms to grow more freely without risk of social conflict, and it may also help minimize the effects of waste products. Irrespective of the reasons for slowed growth, once the worms in high stocking density reached the threshold segment sizes (35–40 segments), they nevertheless formed *vasa*+ clusters similar to the low stocking density worms, as well as similar to the control worms in previous experiments. Therefore, while it took them longer to get to the threshold segment sizes, once they reached the threshold, they displayed similar patterns of gametogenesis. Overall, these results support the segment threshold idea and show that we did not elicit a substantial change in gonial cluster formation patterns in relation with growth state by changing the stocking density condition.

4.4 | Gametogenesis and "counting" segment number

Many annelids regulate and "count" segments they produce, although mechanisms for how they achieve this remain unclear. Polychaetes with indirect development typically have a species-specific number of segments produced in the larvae before hatching (Balavoine, 2014; Blake, 2017), and only after feeding and/or growth cues will they start producing new segments. In the clitellate annelid *Tubifex*, segment

progenitor cells produced during embryogenesis have a birth rank order, and if these progenitors are transplanted in place of "earlier" ranks, they retain their birth rank, suggesting an internal "count" (Kato et al., 2013). Therefore, in *P. dumerilii* we have addressed whether the worms were "counting" the number of segments they have produced, or whether they had to reach an absolute minimum size threshold. We assumed that if *P. dumerilii* juveniles were "counting" the total number of segments produced, with each new segment produced the worms could be growing their head region. This in turn could be triggering the transition into a developmental stage without needing to reach a minimum threshold body size. In other words, it was possible the brain underwent changes with each segment produced, even though worms were overall shorter after amputation. Therefore, the brain could exert an effect towards progressing gametogenesis irrespective of segment number. The effect of hormones produced by the brain on growth and reproduction has been well-studied (Andreatta et al., 2020; Hauenschild, 1966, 1974; Schenk et al., 2016; Schroeder & Hermans, 1975). However, our results support the minimum segment threshold hypothesis as the amputated worms still needed to reach 35–40 segment length for starting to form numerous gonial clusters. Of note, the amputated worms did not experience major differences in their rate of growth compared to controls, but there was a delay in germline development in amputated groups, the longest delays experienced by worms having undergone more severe amputations (P10). The increased lag in the P10 group when compared to the P20 group supports our claim from previous experiments that worms must reach a certain size before the gonial clusters can proliferate.

Unlike ecdysozoans, which have step-function-shaped growth, annelids have continuous asymptotic growth due to continuous segment addition (Sebens, 1987). Developmental transitions such as sexual maturation have been, arguably, easier to study in ecdysozoans because the timing of sexual maturation can be predicted by reaching critical weight and the number of molting events. However, with organisms that show continuous growth such as annelids and planarians it is not as straightforward to predict the timing of a developmental transition based on body size/weight. While *P. dumerilii* is semelparous, and stops growing at maturation, during most of its lifetime, it shows continuous/indeterminate growth. Our work indicates an opportunity to address these questions using segment number as a reliable size/growth metric in *P. dumerilii*, which also has genetic and functional tools available as a research organism.

4.5 | Open questions about the gonial clusters and future directions

This study of systematic characterization of gonial cluster proliferation will help with developmental staging in juveniles for choosing the right individuals (based on segment number) to carry out experiments related to germline and gametogenesis. This will be specifically important for future studies of single cell transcriptomics analyses. Additionally, these results will help improve rearing conditions to maximize animal growth and maturation.

Many questions remain open, mainly on the sources of gonial clusters. Early embryonic origins of PGCs in *P. dumerilii* have been well investigated (Özpolat et al., 2017; Rebscher et al., 2012). In the larvae, there is good evidence that the four PGCs migrate anteriorly behind the jaw region, and then proliferate in this location (Rebscher et al., 2012). There is some evidence via DiI labeling and cell tracing that cells from the anterior cluster migrate to more posterior trunk segments and form the gonial clusters in juvenile worms (Rebscher et al., 2007). However, whether there are *vasa*+ gonial clusters originating from other sources such as locally in the trunk segments or from the posterior growth zone, another region that expresses GMP genes (Gazave et al., 2013) including *vasa*, remains to be addressed. In addition, there is good evidence that the *vasa*+ cell clusters are giving rise to gametes instead of being required for regeneration, but we cannot rule out the possibility that at least some of these cells may have different (non-germline) cell fates. Studies are underway using transgenesis to address these open questions in the future.

ACKNOWLEDGEMENTS

Research reported in this publication was supported by the National Institute of General Medical Sciences of the National Institutes of Health under Award Number R35GM138008 (to BDÖ) and R35GM133420 (to ADW) and Hibbitt Startup Funds (to BDÖ). We thank the Özpolat Lab Members, and many other colleagues who provided their feedback on the manuscript and the preprint.

CONFLICT OF INTERESTS

The authors declare that there are no conflict of interests.

AUTHOR CONTRIBUTIONS

Emily Kuehn: experiments, experiment design, interpretation of results, data analysis, draft. **B. Duygu Özpolat:** experiment design, interpretation of results, data analysis, draft. **David S. Clausen:** data analysis and statistics. **Amy D. Willis**: statistics. **Ryan W. Null**: wrote the HCR oligo generator algorithm. **Ryan W. Null and Bria M. Metzger**: carried out HCRs. All authors have seen and approved the manuscript, and the manuscript has not been accepted or published elsewhere.

DATA AVAILABILITY STATEMENT

The data that support the findings of this study are openly available in GitHub and Zenodo at https://github.com/BDuyguOzpolat/Platynereis-gametogenesis-Kuehn-et-al-2021, https://doi.org/10.5281/zenodo.4587817, https://doi.org/10.5281/zenodo.4587804 (ÖzpolatLab-GitHub-Kuehn, 2021).

ORCID

Ryan W. Null https://orcid.org/0000-0002-3830-4152
Bria M. Metzger https://orcid.org/0000-0002-7721-3034
Amy D. Willis https://orcid.org/0000-0002-2802-4317
B. Duygu Özpolat https://orcid.org/0000-0002-1900-965X

PEER REVIEW

The peer review history for this article is available at https://publons.com/publon/10.1002/jez.b.23100

REFERENCES

Abrevaya, J. (2005). Isotonic quantile regression: asymptotics and bootstrap. *Journal of the Indian Society of Agricultural Statistics*, *67*, 187–199.

Andreatta, G., Broyart, C., Borghgraef, C., Vadiwala, K., Kozin, V., Polo, A., Bileck, A., Beets, I., Schoofs, L., Gerner, C., & Raible, F. (2020). Corazonin signaling integrates energy homeostasis and lunar phase to regulate aspects of growth and sexual maturation in Platynereis. *Proc Natl Acad Sci USA [Internet]*, *117*, 1097–1106. Available from: https://doi.org/10.1073/pnas.1910262116

Balavoine, G. (2014). Segment formation in Annelids: Patterns, processes and evolution. *International Journal of Developmental Biology*, *58*, 469–483.

Biswas, J. K., Sarkar, D., Chakraborty, P., Bhakta, J. N., & Jana, B. B. (2006). Density dependent ambient ammonium as the key factor for optimization of stocking density of common carp in small holding tanks. *Aquaculture*, *261*, 952–959.

Blake, J. A. (2017). Larval development of Polychaeta from the northern California coast. Fourteen additional species together with seasonality of planktic larvae over a 5-year period. *Journal of the Marine Biological Association of the United Kingdom*, *97*, 1081–1133.

Brafield, A. E., & Chapman, G. (1967). Gametogenesis and breeding in a natural population of Nereis Virens. *Journal of the Marine Biological Association of the United Kingdom*, *47*, 619–627.

Choi, H. M. T., Beck, V. A., & Pierce, N. A. (2014). Next-generation in situ hybridization chain reaction: Higher gain, lower cost, greater durability. *ACS Nano*, *8*, 4284–4294.

Choi, H. M. T., Schwarzkopf, M., Fornace, M. E., Acharya, A., Artavanis, G., Stegmaier, J., Cunha, A., & Pierce, N. A. (2018). Third-generation in situ hybridization chain reaction: Multiplexed, quantitative, sensitive, versatile, robust. *Development [Internet]*, *19*, 145. Available from: https://doi.org/10.1242/dev.165753

David, C. N. (2012). Interstitial stem cells in Hydra: Multipotency and decision-making. *International Journal of Developmental Biology*, *56*, 489–497.

Dong, J., Zhao, Y.-Y., Yu, Y.-H., Sun, N., Li, Y.-D., Wei, H., Yang, Z.-Q., Li, X.-D., & Li, L. (2018). Effect of stocking density on growth performance, digestive enzyme activities, and nonspecific immune parameters of Palaemonetes sinensis. *Fish and Shellfish Immunology*, *73*, 37–41.

Fallon, J. F., & Austin, C. R. (1967). Fine structure of gametes of Nereis limbata (Annelida) before and after interaction. *Journal of Experimental Zoology*, *166*, 225–241.

Fischer, A. (1974). Stages and stage distribution in early oogenesis in the Annelid, Platynereis dumerilii. *Cell and Tissue Research*, *156*, 35–45.

Fischer, A. (1975). The structure of symplasmic early oocytes and their enveloping sheath cells in the polychaete, Platynereis dumerilii. *Cell and Tissue Research*, *160*, 327–343.

Fischer, A. H., Henrich, T., & Arendt, D. (2010). The normal development of Platynereis dumerilii (Nereididae, Annelida). *Frontiers in Zoology*, *7*, 31.

García-Alonso, J., Ayoola, J. A. O., Crompton, J., Rebscher, N., & Hardege, J. D. (2011). Development and maturation in the nereidid polychaetes Platynereis dumerilii and Nereis succinea exposed to xenoestrogens. *Comparative Biochemistry And Physiology. Toxicology & pharmacology: CBP*, *154*, 196–203.

Gazave, E., Béhague, J., Laplane, L., Guillou, A., Préau, L., Demilly, A., Balavoine, G., & Vervoort, M. (2013). Posterior elongation in the annelid Platynereis dumerilii involves stem cells molecularly related to primordial germ cells. *Developmental Biology*, *382*, 246–267.

Gehrke, A. R., & Srivastava, M. (2016). Neoblasts and the evolution of whole-body regeneration. *Current Opinion in Genetics & Development*, *40*, 131–137.

Giese, A. C., & Pearse, J., eds. (1974). *Reproduction of Marine Invertebrates —Acoelomate and Pseudocoelomate Metazoans*. Academic Press.

Golding, D. W. (1967). Endocrinology, regeneration and maturation in Nereis. *Biological Bulletin*, *133*, 567–577.

Hariharan, I. K. (2012). How growth abnormalities delay "puberty" in Drosophila. *Science signaling*, *5*, e27.

Hauenschild, C. (1966). Der hormonale einfluss des Gehirns auf die sexuelle Entwicklung bei dem polychaeten Platynereis dumerilii. *General and Comparative Endocrinology*, *6*, 26–73.

Hauenschild, C. (1974). Normalisierung der geschlechtlichen Entwicklung kopfloser Fragmente junger ♀♀ vonPlatynereis dumerilii (Polychaeta) durch Behandlung mit konservierten Prostomien juveniler Individuen. *Helgoländer wissenschaftliche Meeresuntersuchungen*, *26*, 63–81.

Hauenschild, C., & Fischer, A. (1969). *Platynereis dumerilii: mikroskopische Anatomie, Fortpflanzung, Entwicklung*. G. Fischer.

Hempelmann, F. (1911). Zur Naturgeschichte von Nereis dumerilii Aud. et Edw. Available from https://www.schweizerbart.de/publications/detail/artno/169006200/Zur_Naturgeschichte_von_Nereis_dumerilii_Aud_et_Edw

Hofmann, D. K. (1976). Regeneration and endocrinology in the polychaetePlatynereis dumerilii. *Wilhelm Roux's Archives of Developmental Biology*, *180*, 47–71.

Hubbard, E. J. A., Korta, D. Z., & Dalfó, D. (2013). Physiological control of germline development. *Advances in Experimental Medicine and Biology*, *757*, 101–131.

Hutchinson, J. M. C., McNamara, J. M., Houston, A. I., & Vollrath, F. (1997). Dyar's Rule and the Investment Principle: Optimal moulting strategies if feeding rate is size–dependent and growth is discontinuous. *Philosophical Transactions of the Royal Society of London. Series B, Biological Sciences*, *352*, 113–138.

Hyun, S. (2018). Body size regulation by maturation steroid hormones: a Drosophila perspective. *Frontiers in Zoology*, *15*, 44.

Kato, Y., Nakamoto, A., Shiomi, I., Nakao, H., & Shimizu, T. (2013). Primordial germ cells in an oligochaete annelid are specified according to the birth rank order in the mesodermal teloblast lineage. *Developmental Biology*, *379*, 246–257.

Kuehn, E., Stockinger, A. W., Girard, J., Raible, F., & Özpolat, B. D. (2019). A scalable culturing system for the marine annelid Platynereis dumerilii. *PLoS One*, *14*, e0226156.

Lawrence, A. J., & Soame, J. M. (2009). The endocrine control of reproduction in Nereidae: A new multi-hormonal model with implications for their functional role in a changing environment. *Philosophical Transactions of the Royal Society of London. Series B, Biological Sciences*, *364*, 3363–3376.

de Leeuw, J., Hornik, K., & Mair, P. (2009). Isotone optimization in R: Pool-adjacent-violators algorithm (PAVA) and active set methods. *Journal of Statistical Software, Articles*, *32*, 1–24.

Lidke, A. K., Bannister, S., Löwer, A. M., Apel, D. M., Podleschny, M., Kollmann, M., Ackermann, C. F., García-Alonso, J., Raible, F., & Rebscher, N. (2014). 17β-Estradiol induces supernumerary primordial germ cells in embryos of the polychaete Platynereis dumerilii. *General and Comparative Endocrinology*, *196*, 52–61.

Lord, J. P., & Shanks, A. L. (2012). Continuous growth facilitates feeding and reproduction: Impact of size on energy allocation patterns for organisms with indeterminate growth. *Marine Biology volume*, *159*, 1417–1428.

Lui, J. C., & Baron, J. (2011). Mechanisms limiting body growth in mammals. *Endocrine Reviews*, *32*, 422–440.

Meisel, J. (1990). Zur Hormonabhängigkeit der Spermatogenese bei Platynereis dumerilii: licht-und elektronenmikroskopische Befunde sowie experimentelle Untersuchungen in vivo und in vitro. na.

Michaelson, D., Korta, D. Z., Capua, Y., & Hubbard, E. J. A. (2010). Insulin signaling promotes germline proliferation in C. elegans. *Development*, *137*, 671–680.

Narbonne, P., & Roy, R. (2006). Regulation of germline stem cell proliferation downstream of nutrient sensing. *Cell Division*, *1*, 29.

Nieuwkoop, P. D., & Sutasurya, L. A. (1979). *Primordial Germ Cells in the Chordates: Embryogenesis and Phylogenesis*. Cambridge University Press.

Nieuwkoop, P. D., & Sutasurya, L. A. (1981). *Primordial Germ Cells in the Invertebrates: From Epigenesis to Preformation*. Cambridge University Press.

Özpolat, B. D., Handberg-Thorsager, M., Vervoort, M., & Balavoine, G. (2017). Cell lineage and cell cycling analyses of the 4d micromere using live imaging in the marine annelid platynereis dumerilii. *Elife*, *6*, e30463. https://doi.org/10.7554/eLife.30463

Özpolat, B. D., Randel, N., Williams, E. A., Bezares-Calderón, L. A., Andreatta, G., Balavoine, G., Bertucci, P. Y., Ferrier, D. E. K., Gambi, M. C., Gazave, E., Handberg-Thorsager, M., Hardege, J., Hird, C., Hsieh, Y.-W., Hui, J., Mutemi, K. N., Schneider, S. Q., Simakov, O., Vergara, H. M., … Arendt, D. (2021). The Nereid on the rise: Platynereis as a model system. *EvoDevo*, *12*, 10.

ÖzpolatLab-GitHub-Kuehn. (2021). R codes, protocols, additional files on Github for Kuehn et al 2021. Github. Available from: https://github.com/BDuyguOzpolat/Platynereis-gametogenesis-Kuehn-et-al-2021

ÖzpolatLab-HCR. (2021). Özpolat Lab HCR probe generator. Github. Available from: https://github.com/rwnull/insitu_probe_generator

Plaistow, S. J., Lapsley, C. T., Beckerman, A. P., & Benton, T. G. (2004). Age and size at maturity: Sex, environmental variability and developmental thresholds. *Proceedings. Biological sciences/The Royal Society*, *271*, 919–924.

R Core Team. (2020). R: A Language and Environment for Statistical Computing. Available from: https://www.R-project.org/

Rebscher, N. (2014). Establishing the germline in spiralian embyos. *International Journal of Developmental Biology*, *58*, 403–411.

Rebscher, N., Lidke, A. K., & Ackermann, C. F. (2012). Hidden in the crowd: Primordial germ cells and somatic stem cells in the mesodermal posterior growth zone of the polychaete Platynereis dumerillii are two distinct cell populations. *EvoDevo*, *3*, 9.

Rebscher, N., Zelada-González, F., Banisch, T. U., Raible, F., & Arendt, D. (2007). Vasa unveils a common origin of germ cells and of somatic stem cells from the posterior growth zone in the polychaete Platynereis dumerilii. *Developmental Biology*, *306*, 599–611.

RStudio Team. (2020). RStudio: Integrated Development Environment for R. Available from: http://www.rstudio.com/

Schenk, S., Bannister, S. C., Sedlazeck, F. J., Anrather, D., Minh, B. Q., Bileck, A., Hartl, M., von Haeseler, A., Gerner, C., Raible, F., & Tessmar-Raible, K. (2019). Combined transcriptome and proteome profiling reveals specific molecular brain signatures for sex, maturation and circalunar clock phase. *Elife*, *8*, e41556. https://doi.org/10.7554/eLife.41556

Schenk, S., Krauditsch, C., Frühauf, P., Gerner, C., & Raible, F. 2016. Discovery of methylfarnesoate as the annelid brain hormone reveals an ancient role of sesquiterpenoids in reproduction. *Elife*, *[Internet]*,5. Available from: https://doi.org/10.7554/eLife.17126

Schindelin, J., Arganda-Carreras, I., Frise, E., Kaynig, V., Longair, M., Pietzsch, T., Preibisch, S., Rueden, C., Saalfeld, S., Schmid, B., Tinevez, J.-Y., White, D. J., Hartenstein, V., Eliceiri, K., Tomancak, P., & Cardona, A. (2012). Fiji: An open-source platform for biological-image analysis. *Nature Methods*, *9*, 676–682.

Schroeder, P. C., & Hermans, C. O. (1975). Annelida: Polychaeta. In editors Giese, A. C. & Pearse, J. S., *Reproduction of Marine Invertebrates. Vol. 3: Annelids and Echiurans*. Academic Press.

Sebens, K. P. (1987). The ecology of indeterminate growth in animals. *Annual Review of Ecology and Systematics*, *18*, 371–407.

Shibata, N., Umesono, Y., Orii, H., Sakurai, T., Watanabe, K., & Agata, K. (1999). Expression of vasa(vas)-related genes in germline cells and totipotent somatic stem cells of planarians. *Developmental Biology*, *206*, 73–87.

Shim, J., Gururaja-Rao, S., & Banerjee, U. (2013). Nutritional regulation of stem and progenitor cells in Drosophila. *Development*, *140*, 4647–4656.

Tennessen, J. M., & Thummel, C. S. (2011). Coordinating growth and maturation—insights from Drosophila. *Current Biology*, *21*, R750–R757.

Tettelbach, S. T., Barnes, D., Aldred, J., Rivara, G., Bonal, D., Weinstock, A., Fitzsimons-Diaz, C., Thiel, J., Cammarota, M. C., Stark, A., Wejnert, K., Ames, R., & Carroll, J. (2011). Utility of high-density plantings in bay scallop, Argopecten irradians irradians, restoration. *Aquac Int*, *19*, 715–739.

Tharp, M. E., Collins, J. J., 3rd, & Newmark, P. A. (2014). A lophotrochozoan-specific nuclear hormone receptor is required for reproductive system development in the planarian. *Developmental Biology*, *396*, 150–157.

Zelada González, Y. F. (2005). Germline development in Platynereis dumerilii and its connection to embryonic patterning. Available from: http://archiv.ub.uni-heidelberg.de/volltextserver/5432/

SUPPORTING INFORMATION

Additional supporting information may be found in the online version of the article at the publisher's website.

How to cite this article: Kuehn, E., Clausen, D. S., Null, R. W., Metzger, B. M., Willis, A. D., & Özpolat, B. D. (2022). Segment number threshold determines juvenile onset of germline cluster expansion in *Platynereis dumerilii*. *Journal of Experimental Zoology Part B: Molecular and Developmental Evolution*, 338, 225–240. https://doi.org/10.1002/jez.b.23100